Supramolecular Room-Temperature Phosphorescent Hydrogels based on hexamethylcucurbit[5]uril for Cell Imaging

Xi-Ran Sun [a], Shuai Zhang [a], Ming Liu [a], Xi Zeng [a,*] Carl Redshaw [b], Zhu Tao [a], Xin Xiao [a*]

[a] *Key Laboratory of Macrocyclic and Supramolecular Chemistry of Guizhou Province, Applied Chemistry, Guizhou University, Guizhou University, Guiyang 550025, China.*

[b] *Department of Chemistry, University of Hull, Hull HU6 7RX, U.K.*

Abstract: The host-guest interaction between hexamethylcucurbit[5]uril (HmeQ[5]) and 1,4-diaminobenzene (DB) was investigated, and a new low molecular weight supramolecular gel was prepared by a simple heating/mixing cooling method. The structure and properties of the supramolecular gel were characterized. Results revealed that DB molecules did not enter the cavity of HmeQ[5], and that hydrogen bonding between the carbonyl group at the HmeQ[5] port and the DB amino groups, together with dipole dipole interactions and outer wall interactions were the main driving forces for the formation of the supramolecular gel. The HmeQ[5]/DB gel system exhibits temperature sensitivity. The phosphor 6-bromo-2-naphthol (BrNp) was embedded in the gel to give the gel fluorescent phosphorescence double emission. The double emission ability at room temperature can be attributed to the ordered microstructure of the supramolecular gel, which effectively avoids the non-radiative transition of BrNp. The analytical properties of the gel system were determined, and the results showed that it had potential application in the detection of trace BrNp. In the range of 1.0×10^{-6} mol·L^{-1}~1.0×10^{-4} mol·L^{-1}, the RTP intensity was linear with respect to the concentration of BrNp; the detection limit is 95 nmol/L. This work shows that the HmeQ[5]/DB gel, as a structural platform for inducing phosphorescence, has potential application value in new phosphorescent soft materials.

Keywords: host–guest self-assembly, cucurbit[*n*]urils, 1,4-diaminobenzene, supramolecular hydrogel, room-temperature phosphorescence, 6-bromo-2-naphthol

1. Introduction

Hydrogels are a kind of inherent hydrated polymeric network material prepared by three-dimensional crosslinking of hydrophilic polymers. [1] They have physical properties similar to soft biological tissues and can hold a large amount of water through surface tension or capillary effects. Therefore, they are widely used as important materials in biomedical and other fields. [2] The preparation of hydrogel materials has two crosslinking modes: covalent and non-covalent. [3] Covalent crosslinking usually provides relatively brittle chemical hydrogels. If the crosslinking network is destroyed, the hydrogel is difficult to biodegrade and lacks the ability of self-healing, which limits its application in various biomedical applications.

Supramolecular gels are a new kind of three-dimensional crosslinked network polymer material formed by the self-assembly of small molecules under the influence of various non-covalent interactions. They perfectly combine the advantages of synthetic hydrogels and supramolecular polymers. [5 – 8] They not only have unique physical and chemical properties (such as water retention capacity, drug loading capacity, biodegradability and biocompatibility, biological stability) and inherent processability of the supramolecular crosslinking units, [9] but also exhibit reversible gel-sol transition behavior in response to various biological related stimuli. [10] They can be used as an intelligent carrier to deliver a variety of therapeutic agents (such as drugs, genes, proteins) and as a promising matrix to repair and regenerate human tissues and organs, and show great potential as biomaterial scaffolds for diagnosis and treatment.

In supramolecular hydrogels, cucurbit[*n*]urils (n=5-10), as a new generation of supramolecular macrocyclic host molecule, have become a good platform for the construction of such supramolecular hydrogels. [8] They have a unique central hydrophobic cavity, two polar carbonyl ports with negative electrostatic potential and a circular outer surface with positive electrostatic potential. They can selectively interact with guest molecules to form complexes. This host-guest interaction is weak and reversible, so it is sensitive to external stimuli such as temperature and pH, which will lead to different supramolecular structures and properties. [9] At present, there are three main reported construction methods for cucurbit[*n*]uril-based hydrogels: 1. The cucurbit[*n*]uril [n=8,10] is mainly used as a cross-linking agent, whereby the large cavity is used to combine two or three guest molecules at the same time to form ternary or quaternary complexes, so as to realize the cross-linking of supramolecules and construct supramolecular hydrogels. [10] 2. To functionalize cucurbit[*n*]uril and

synthesize cucurbit[*n*]uril modified polymers. Through the host-guest interactions between the cucurbit[*n*]uril and the corresponding guest molecules on the polymer, the gel system can be constructed. [11] 3. To construct a gel system with cucurbit[*n*]uril as a small molecular unit. [12] The driving force of aggregation to form hydrogels is mainly the use of strong hydrogen bonds between the cucurbit[*n*]uril ports and water/ions, dipole interactions between cucurbit[*n*]uril molecules under appropriate acidic conditions, and self-assembly to form nanofibers. This last method is rarely reported at present.

Organic room temperature phosphorescence (ORTP) materials have attracted much attention because of their long life, large Stokes displacement and strong anti-interference ability [13a~e], and have potential application in anti-counterfeiting, sensing, displays, data loading and so on. It is particularly noteworthy that ORTP materials can maintain strong continuous emission after removing external excitation, and their time-resolved imaging can effectively avoid spontaneous fluorescence and scattered light. Given they have the characteristics of anti-background fluorescence interference, for biological imaging such as clinical diagnosis [14] and tumor treatment [15], they have become an important auxiliary tool to understand the mechanisms of various physiological processes [16]. The combination of supramolecular hydrogels and organic room temperature phosphors is an important direction for the preparation of new soft materials.

In this paper, cucurbit[5]uril-based hydrogels were constructed by the supramolecular self-assembly of the small molecular compounds hexamethylcucurbit[5]uril (HmeQ[5]) and 1,4-diaminobenzene (DB) through a supramolecular self-assembly, driven by non-covalent interactions such as hydrogen bonds, dipole interactions and external surface interactions. The structure and morphology of the supramolecular hydrogel were characterized by NMR, UV-Vis, fluorescence, phosphorescence spectra, scanning electron microscopy, rheometer, etc. The temperature sensitivity of the HmeQ[5]/DB hydrogel system was studied. Based on this matrix, 6-bromo-2-naphthol (BrNp) phosphors were embedded in the three-dimensional gel network. The mechanism of supermolecular gel inducing BrNp to produce RTP and the structural reversible RTP property changes of the gel system were studied, and the analytical performance of the HmeQ[5]/DB-RTP system was investigated. This work provides basic research for expanding the application of cucurbit[*n*]urils and preparing new soft materials for phosphorescence emission.

2. Experimental Section

2.1 *Materials*: The compound hexamethylcucurbit[5]uril (HmeQ[5]) was synthesized according to the literature procedure. [18] Other reagents and chemicals were obtained from Innochem (Beijing, China) and Aladdin (Shanghai, China). All reagents were analytical reagent grade and used without further purification. Double distilled water was used throughout.

2.2 *Characterization methods*: Titration ^{1}H nuclear magnetic resonance (^{1}H NMR) experiments were determined at 400 MHz on a JEOL JNM-ECZ400s spectrometer. Inverted fluorescence microscope (IFM) images were performed on a Nikon Eclipse Ti-S fluorescent inverted microscope. Dynamic light scattering (DLS) analyses were conducted on a laser light scattering spectrometer (BI-200SM) equipped with a digital correlator (BI-9000AT) at 25 °C. SEM observations were carried out using a Hitachi SU8010 field emission SEM system. Samples were deposited on a SiO_2/Si substrate, and then lyophilized or dried at room temperature. Dynamic oscillatory rheological characterization was performed with a Mars 40 （Thermo Scientific, USA） controlled strain rheometer at 25 °C. Crystal data were collected on a Bruker D8 Venture X-ray single crystal diffraction using graphite monochromatic Mo-K ray (λ = 0.71 073 Å, μ = 0.828 mm^{-1}) in ω-scan mode. Lorentz polarization and absorption corrections were applied. Structural solution and full matrix least-squares refinement based on *F*2 were performed with the SHELXS-97 and SHELXL-97 program package, respectively. All nonhydrogen atoms were refined anisotropically. Analytical expressions of the neutral-atom scattering factors were employed and anomalous dispersion corrections were incorporated. UV–vis spectra were obtained on a UV-2700 dual-beam UV–vis spectrophotometer (Shimadzu Instruments Co. Ltd.). Fluorescence/phosphorescence spectra, RTP spectra recorded on a Cary Eclipse Fluorescence/phosphorescence Spectrometer (Varian, USA). Phosphorescence mode; Excitation slit = 20 nm; Emission slit = 20 nm; Delay time = 0.2 ms; Gate time = 2.0 ms; Laser scanning confocal microscope images were obtained on ZEISS LSM 900.

3. Results and discussion

3.1 *Construction and characterization of the HmeQ[5]/DB hydrogel*

The HmeQ[5]/DB hydrogel was prepared by simply heating a formic acid aqueous solution of mixed HmeQ[5] (0.46-1.83 wt%) and DB (0.14-0.58 wt%). The transparent solution can be slowly cooled at room temperature to form hydrogels. The optimization results show that hydrogels (2 ml, figure S1, supporting information) can be obtained over the concentration range using HmeQ[5] and DB with 0.46-1.83 and 0.14-0.58wt%, respectively. Further experimental results show that addition

of more HmeQ[5] and DB is not necessarily beneficial. The mixture of HmeQ[5] and DB with 1.14 wt% and 0.36wt% respectively can produce a more solidified hydrogel in formic acid solution (Figure S1, supporting information). It is worth noting that in formic acid medium, the gel speed can be controlled by adjusting the water content. Under the above optimized conditions, controlling the formic acid: water =1:9, v/v gel takes only 1 h (Table S2). Therefore, we speculate that the protonation of the DB guest plays an important role in the gel process. Under acidic conditions, the amino protonation of the DB guest further strengthens the interaction with the carbonyl oxygen atom at the port of the HmeQ[5] host. This interaction includes not only the hydrogen bond and ion dipole interaction between the protonated amine group and the terminal carbonyl oxygen atom, but also outer wall interactions between HmeQ[5] and the guest.

To confirm the role of HmeQ[5] and DB in the formation of the supramolecular gel, ^{1}H NMR spectra of the gel were recorded (Figure S2). The ^{1}H NMR titration spectra of HmeQ[5] showed that after addition of DB, there was a continuous decrease in the strength of the proton signal of HmeQ[5]. However, no proton resonances corresponding to DB were detected (Figures S5a–c, Supporting Information). When the molar ratio of HmeQ[5] to DB reached 1:1, all proton resonances attributed to the relevant components in the ^{1}H NMR spectrum seemed to disappear (Figure S1, Supporting Information). Upon further addition of DB, only increased proton resonances ascribed to DB were detected. The proton signal of DB never exhibited a high field shift, indicating that DB does not enter the cavity of HmeQ[5]. During the whole titration process, the system was a clear solution, and the results suggested that the formation of a supramolecular self-assembly between the HmeQ[5] host and the DB guest occurred with a ratio of 1:1.

Then, we studied the host-guest interaction between HmeQ[5] and DB by UV-vis spectroscopy. It can be seen from Figure S2 that the DB solution has two absorption bands at 234 nm and 285 nm, corresponding to the $\pi \rightarrow \pi^*$ transition and $n \rightarrow \pi^*$ transition of DB, respectively. With the addition of HmeQ[5] at different molar ratios, the 234 nm absorption band first gradually weakened, then rapidly blue shifted and significantly enhanced, while the 285 nm absorption band gradually weakened. When HmeQ[5] was added at the molar ratio of 1:1, the intensity remained basically constant. At the same time, an equal absorption point appears at 315 nm. This shows that DB interacts with HmeQ[5] to form a complex, and according to the molar ratio method, the binding ratio of the two is 1:1 (Figure 1).

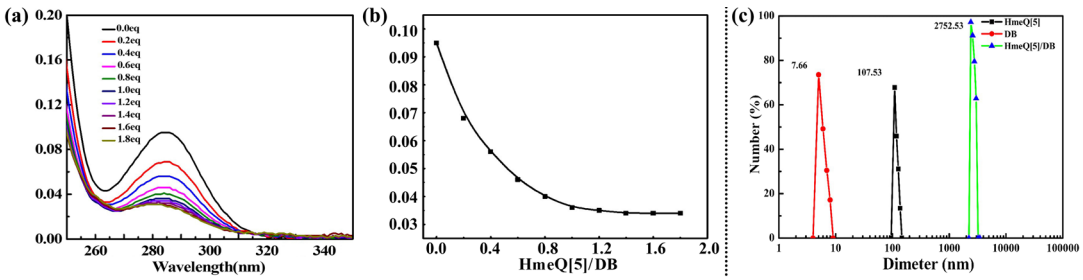

Figure 1. Absorption spectral titrations of DB with HmeQ[5] (DB, 10 μM, HCOOH/H_2O=1/9, v/v) (a), the variation of absorption intensity against the number of equivalents of HmeQ[5] (b), DLS data of HmeQ[5]/DB (c) (0.5 mM, HCOOH/H_2O=1/9, v/v).

Dynamic light scattering (DLS) in formic acid aqueous solution has been used to monitor the formation of supramolecular assemblies based on HmeQ[5]/DB. Figure 1c in the ESI shows the DLS data for the HmeQ[5]/DB based supramolecular assembly in HCOOH aqueous solution. The experimental results show that by mixing HmeQ[5] and DB in a molar ratio of 1:1 (5.0 mm), a hydrodynamic diameter distribution centered at 2752 nm in HCOOH medium can be observed, indicating that the aggregates with average particle size are formed under experimental conditions, which provides indirect evidence for the supramolecular self-assembly solution structure between HmeQ[5] and DB.

HmeQ[5] is the smallest cucurbit[*n*]uril. Its cavity can only contain gas molecules, but organic molecules cannot enter, however HmeQ[5] has two ports surrounded by carbonyl groups. The hydrogen bonding, dipole and external surface interactions between it and the amino group of the protonated diaminobenzene play an important role in the self-assembly process. The morphology and structure of the HmeQ[5]/DB hydrogel formed in HCOOH medium were investigated by scanning electron microscopy (SEM). SEM shows the morphology of the freeze-dried hydrogel (Figure 2), and the image clearly shows the fibrous network. It consists of fibers with corresponding length up to hundreds of microns, which are composed of bundles of fibrils and form hydrogels. The formation of fibers in the gel shows that the self-assembly is driven by strong directional intermolecular interactions. The formation of supramolecular chain between the HmeQ[5]/DB guest was further confirmed.

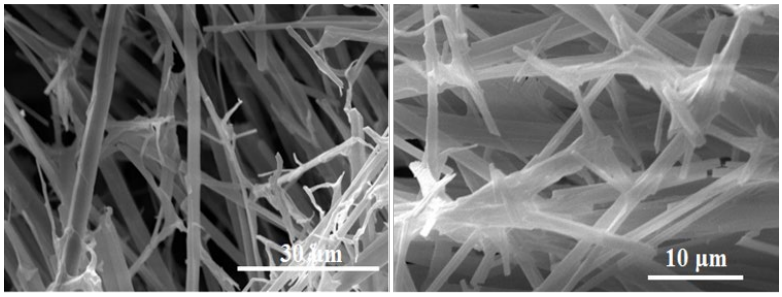

Figure 2. SEM images of the HmeQ[5]/DB hydrogel.

The mechanical properties of the HmeQ[5]/DB based hydrogels were characterized by rheometer measurements. Strain dependent oscillatory rheology (Figures 3a-d) shows a relatively wide linear viscoelastic region. The linear viscoelasticity of the HmeQ[5]/DB hydrogel in HCOOH medium is ≈ 37% strain. Above this critical yield strain, the network breaks down, which can be observed by the sharp decline of modulus and the inversion of the viscoelastic signal (G″>G′). This shows that the construction of the mechanical connection network based on HmeQ[5]/DB is sensitive to shear and behaves in a highly viscoelastic manner with the increase of angular frequency. In the frequency scanning of the HmeQ[5]/DB hydrogel network (Figures 3b and 3d), over the whole measured frequency range, the elastic modulus (G′) is higher than the loss modulus (G″), while G' and G″ are relatively independent of frequency. Furthermore, thixotropic ring experiment is used to detect the structural resilience. The difference (D-value) between the upper rheological integral area and the lower rheological integral area is 1042.965 Pa/s (Figure 3e), indicating that this supramolecular gel is susceptible to external force denaturation. At the same time, the viscosity of upper and lower flow ramp (η) is almost completely coincident, indicating that the supramolecular gel has almost no thixotropy (Figure 3f).

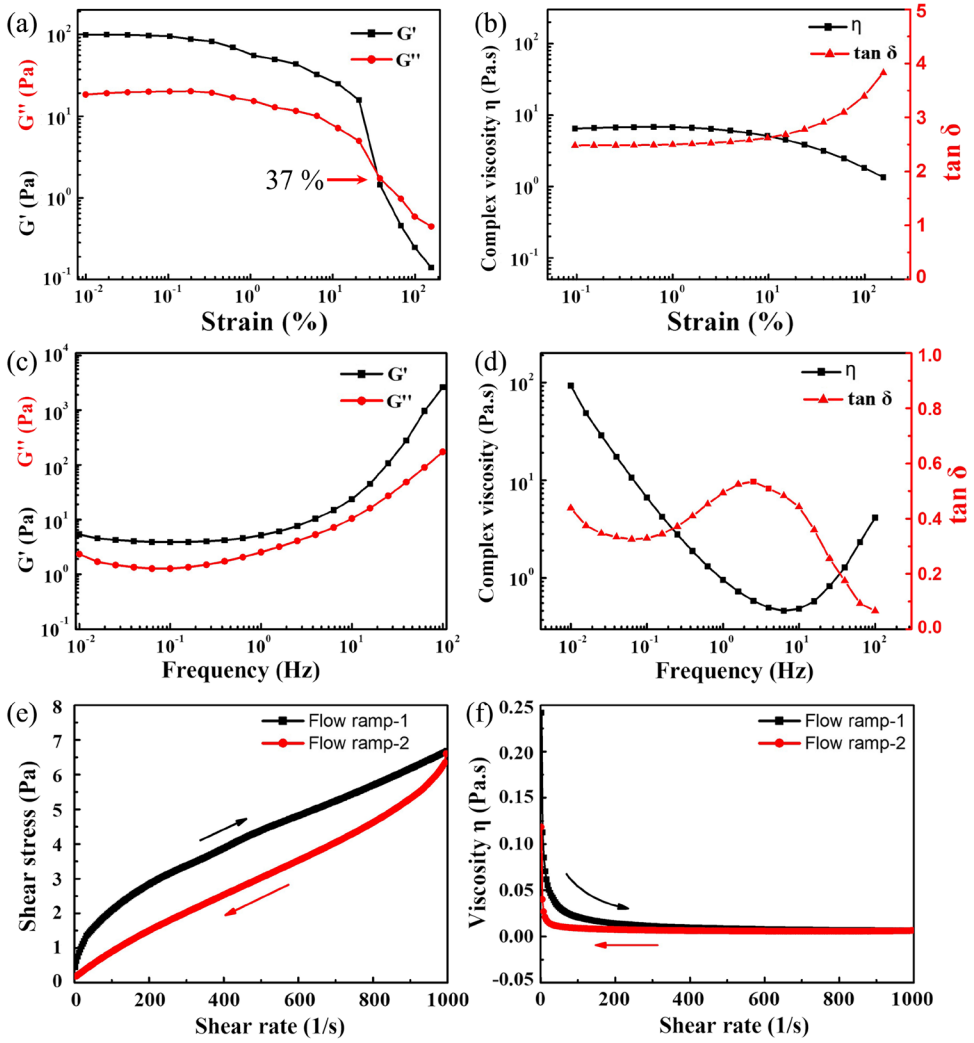

Figure 3. Dynamic oscillatory rheological characterization of HmeQ[5]/DB-based hydrogels prepared in this study conducted at 25 °C: a) Storage and loss modulus obtained from the strain amplitude sweep measurements; b) complex viscosity and tan *δ* obtained from the strain amplitude sweep measurements; c) Storage and loss modulus obtained from the frequency sweep measurements; d) complex viscosity and tan *δ* obtained from the frequency sweep measurements; e) the curve of shear stress *versus* shear rate; f) the viscosity η Curve graph of change with shear rate.

We further studied the stimulus response behavior of the thermoreversible gel sol transition of HmeQ[5] in the presence of equimolar amounts of the DB guest in formic acid aqueous solution (formic acid: water =1:9, v/v). When the HmeQ[5]/DB gel was cooled to about 25℃, the transition from sol to gel was observed, while when heated, the slow transition from gel to sol was observed within the temperature range of 76 ℃ (Figure 4).

Figure 4. Sol-gel phase transition of the HmeQ[5]/DB gel.

In order to more fully understand the molecular structure that leads to the formation of the gel, we prepared a suitable sample and determined the X-ray crystal structure of acicular crystals by diluting and dissolving the formed HmeQ[5]/DB hydrogel with water and then slowly volatilizing it. [11] As shown in Figure 5, careful examination of the crystal structure shows that under acidic conditions, the DB molecules form $-NH_3^+$, the three hydrogen atoms on nitrogen form C-H ·· O=C hydrogen bonds with carbonyl at the symmetrical center of HmeQ[5], while nitrogen positive ions form dipole interactions with negatively charged oxygen atoms of carbonyl. DB ions act as "adhesives" to combine HmeQ[5] molecules through C-H ·· O=C hydrogen bonds and C=O···N^+ ion-dipole interactions between oxygen atoms of the carbonyl fringed portals of HmeQ[5], and the unit is assembled into a long fiber. At the same time, each long fiber is staggered, and the units are bunched into coarse fibers through the action of the outer surface interactions [17] between the methyl groups of HmeQ[5] and the DB benzene ring, forming a fiber network and forming a gel.

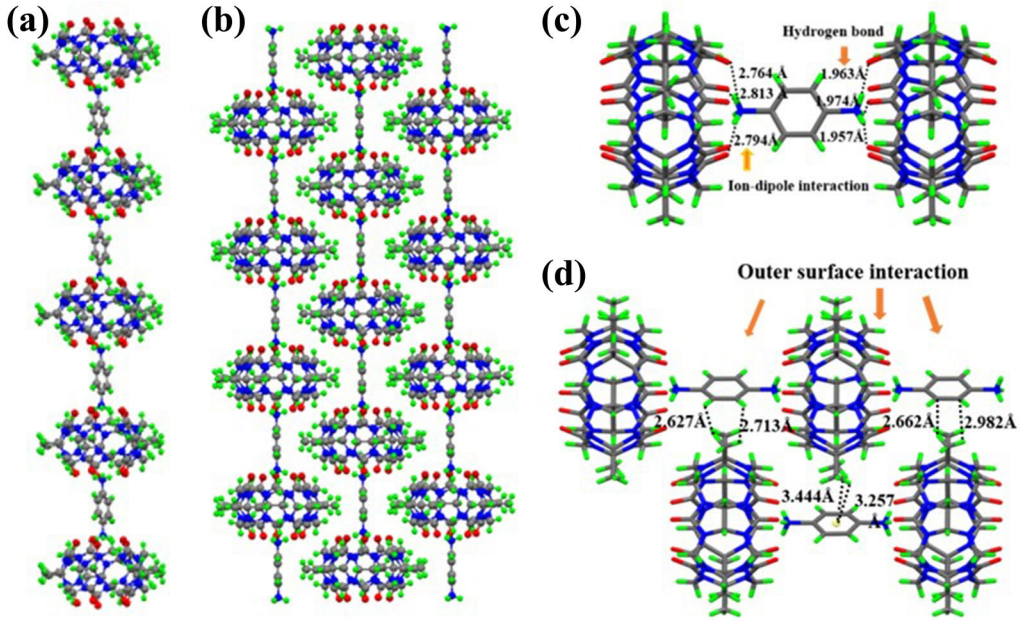

Figure 5. Crystal structure of a) HmeQ[5]/DB-based framework constructed by b) 1D supramolecular chain formed from alternating molecules of HmeQ[5] and DB; c) detailed interactions between HmeQ[5] and DB; d) interactions formed between the HmeQ[5]/DB -based supramolecular chains.

3.2 **Preparation of Supramolecular Gels with BrNp.**

The phosphor **BrNp** and HmeQ[5]/DB gel were dissolved in aqueous formic acid solution ($HCOOH/H_2O$, 1/9, v/v) and heated to 80 ℃ in an oil bath. The mixture was then cooled to room temperature to form a stable gel (expressed as HmeQ[5]/DB gel). The mass fractions of HmeQ[5]/DB and **BrNp** in all samples were 1.50 wt % and 1×10^{-4} $mol\cdot L^{-1}$, respectively. Deoxidation is not required during sample preparation. Furthermore, we studied the influence of the concentration of HmeQ[5]/DB on the room temperature phosphorescence of **BrNp** (Figure S5), and the influence of the solvent formic acid/water ratio on the room temperature phosphorescence of **BrNp** (Figure S6). Since it takes a certain time for **BrNp** to generate phosphorescence in the HmeQ[5]/DB supramolecular gel, we explored **BrNp** (1.0 × 10-4 mol / L) in this gel (0.025 mol / L, formic acid / water = 1 / 9, V / V). As shown in Figures 6 a, b), it can be seen from this figure that when the storage time reaches 8 h, a phosphorescent signal starts to be sent out, and then the phosphorescent intensity gradually increases. When the storage time reaches 24 h, the phosphorescent intensity reaches the maximum, and then tends to be stable. With the increase of the storage time, the supramolecular gel gradually turns white (as shown in Figures 6c and S7-S8). With the deepening of the whiteness of the supramolecular gel, the RTP of **BrNp** increases, until the whiteness of the supramolecular gel no longer increases and the RTP tends to be stable. Finally the best condition was obtained: the concentration of HmeQ[5]/DB is 0.025 mol/L and the solvent formic acid/water ratio is 1/9 (formic acid/water, v/v), the phosphorescence emission of **BrNp** is good after being placed for 30 h.

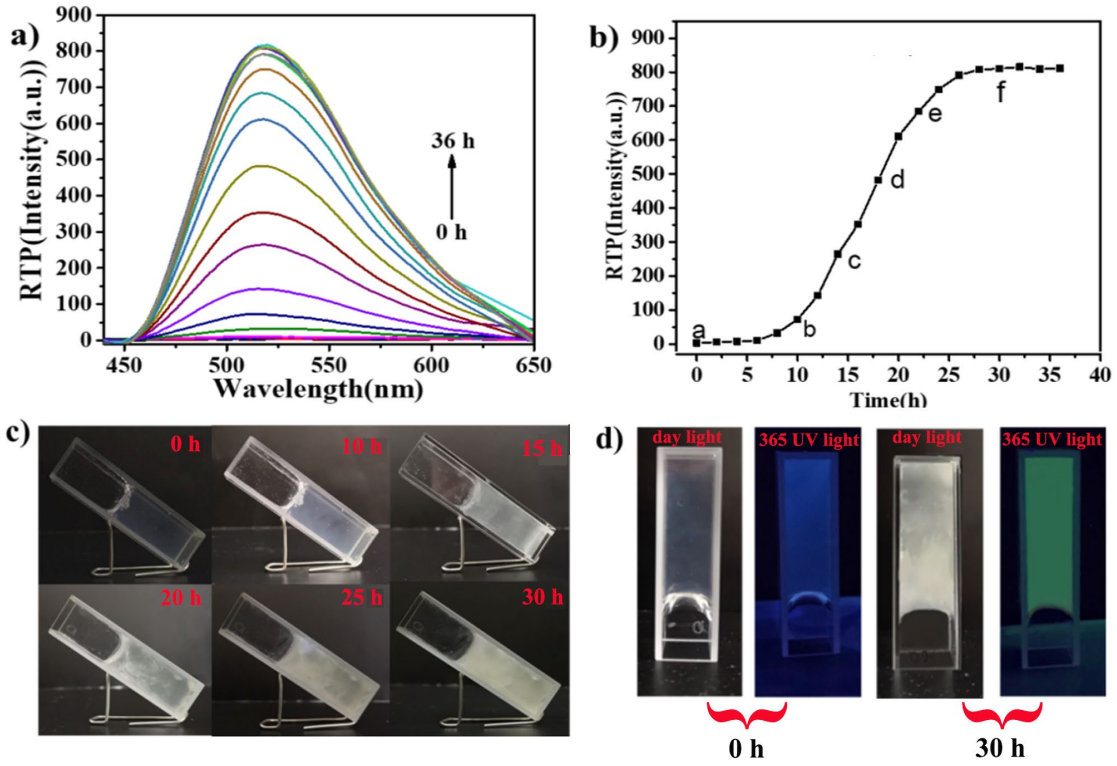

Figure 6 a) The phosphorescent spectrum of the supramolecular gel HmeQ[5]/DB-**BrNp** (**BrNp**, 1.0×10^{-4} mol / L) at different storage times, b) Curve of change of phosphorescent intensity and storage time at 520 nm, c) Photos of supramolecular gel HmeQ[5]/DB-**BrNp** placed at different times, d) Photos of supramolecular gel HmeQ[5]/DB-**BrNp** under sunlight and 365nm ultraviolet lamp at 0h and 30h.

Throughout the above process, the solvent molecules are immobilized in the 3D network structure, resulting in the system gel [18]. As shown in Figure S4, the gel system shows stimulation to heat. The thermal response comes from the inherent structural thermal reversibility of the supramolecular gel. The expression of these reactions is the sol-gel phase transition of the system. **BrNp** is a typical luminescent molecule, and due to the long lifetime of excited triplet molecules, the luminescence of **BrNp** is usually quenched by collision with surrounding solvent molecules or itself. At this time, **BrNp** in the solution should emit fluorescence, but cannot emit room temperature phosphorescence (RTP). When **BrNp** is dispersed in the above gel state, the ordered structure of the HmeQ[5]/DB gel plays a role in stabilizing **BrNp**, effectively avoiding non radiative transition, and it is expected to emit RTP and fluorescence (FL) at the same time. Therefore, under certain stimulation, when the gelatinous state changes to the colloidal state, the **BrNp** dispersed in the system will break away from the ordered structure. If the original structure of the HmeQ[5]/DB is restored, then the gel

state can be reconstructed. These reactions are reversible, which endows the gel system with reversible double emission.

In order to confirm the above hypothesis, we conducted FL and RTP spectroscopic studies on the thermal reversibility of the HmeQ[5]/DB-**BrNp** gel. The emission intensity of **BrNp** loaded on the hydrogel was measured over the temperature range 25-80℃. As shown in Figures 7a-b, the freshly heated solution/sol is excited by 335 nm ultraviolet light. Without deoxidation, the high-intensity FL emission of the 367 nm sample exhibits blue fluorescence under the irradiation of 365nm ultraviolet lamp. However, with the decrease of temperature, the gel phase is gradually formed and the fluorescence intensity is gradually weakened (Figure 7), which shows that the **BrNp** is exposed to a more hydrophilic environment as the gel phase changes to the solution/sol phase. At the same time, in the cooling cycle, when the temperature drops from 70 ℃ to 25 ℃, under the irradiation of 315 nm UV lamp, there is a new peak at 550 nm, and the emission intensity gradually increases with the formation of the gel.

After the gel is completely formed, the strength basically remains unchanged. **BrNp** is a hydrophobic compound, which is likely to exist in the ordered structure of the HmeQ[5]/DB fiber aggregates. This shows that **BrNp** is dispersed in the hydrophobic micro region composed of the HmeQ[5]/DB fiber aggregates, avoiding the non-radiative transition of **BrNp**, and the 3D network structure formed by the HmeQ[5]/DB fiber aggregates plays a key role in the dual emission of **BrNp**. The lifetime of RTP and FL is 0.135 ms (Figure S10), proved by the imaging study using laser confocal microscopy (Figure 7e). The microscope without **BrNp** cannot observed the emission in the 404 nm channel, while the gel fiber with **BrNp** emits turquoise phosphorescence, and the emission life of light is 0.135 ms, which also confirms the emission of phosphorescence.

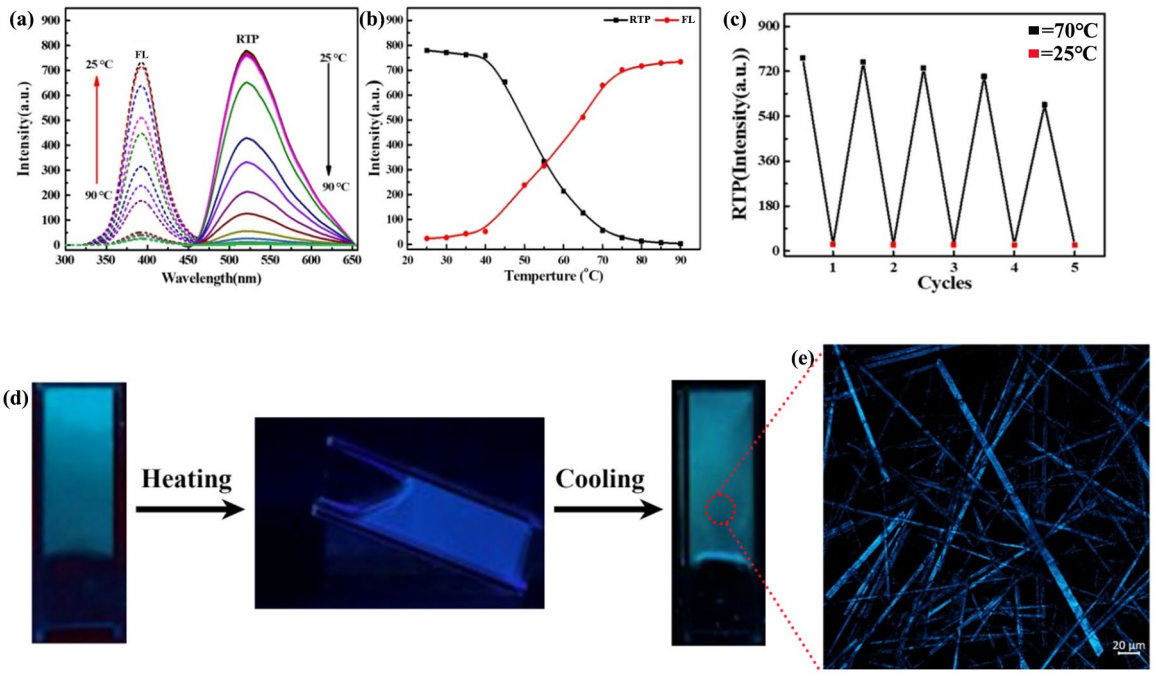

Figure 7 a) Fluorescence and phosphorescence spectra at different temperatures, b) Variation of fluorescence and phosphorescence intensity *versus* temperature, c) Phosphorescence data of supramolecular gel HmeQ[5]/DB-**BrNp** at 70 ℃ and 25 ℃ for 5 cycles, d) Sol-gel phase transition of the HmeQ[5]/DB-**BrNp** supramolecular gel under 365nm ultraviolet lamp, e) Laser confocal image of supramolecular gel HmeQ[5]/DB-**BrNp** (channel: 404 nm).

The luminescence analysis performance of the gel system was tested. In the HmeQ[5]/DB supramolecular gel system, the concentration of **BrNp** was changed, and the change rule of room temperature phosphorescence intensity with **BrNp** concentration was determined. In Figure 8, the phosphorescence intensity first increased and then slightly decreased with the increase of **BrNp** concentration. When the **BrNp** concentration reached 2.0×10^{-4} mol·L^{-1}, the phosphorescence intensity reached the maximum value. When the **BrNp** concentration exceeds 2.0×10^{-4} mol/l, **BrNp** may be quenched due to excessive concentration, resulting in a decrease in phosphorescence intensity. The results showed that for the concentration of **BrNp** between 1.0×10^{-6} mol·L^{-1} - 1.0×10^{-5} mol·L^{-1} and 1.0×10^{-5} mol·L^{-1}-1.0×10^{-4} mol·L^{-1}, there is a linear relationship and the correlation coefficients are 0.9977 and 0.9987 respectively, indicating that there is a good linear relationship between the concentration of **BrNp** and the phosphorescence emission intensity of the HmeQ[5]/DB supramolecular gel over these two concentration ranges. On repeating the determination of a blank gel for 10 times, the calculated standard deviation is 0.497. Using the formula l=3s/k (k is the slope of the regression equation), the detection limit is 95 nm. It can be seen that **BrNp** has good room

temperature phosphorescence detection and analysis parameters in the HmeQ[5]/DB supramolecular gel.

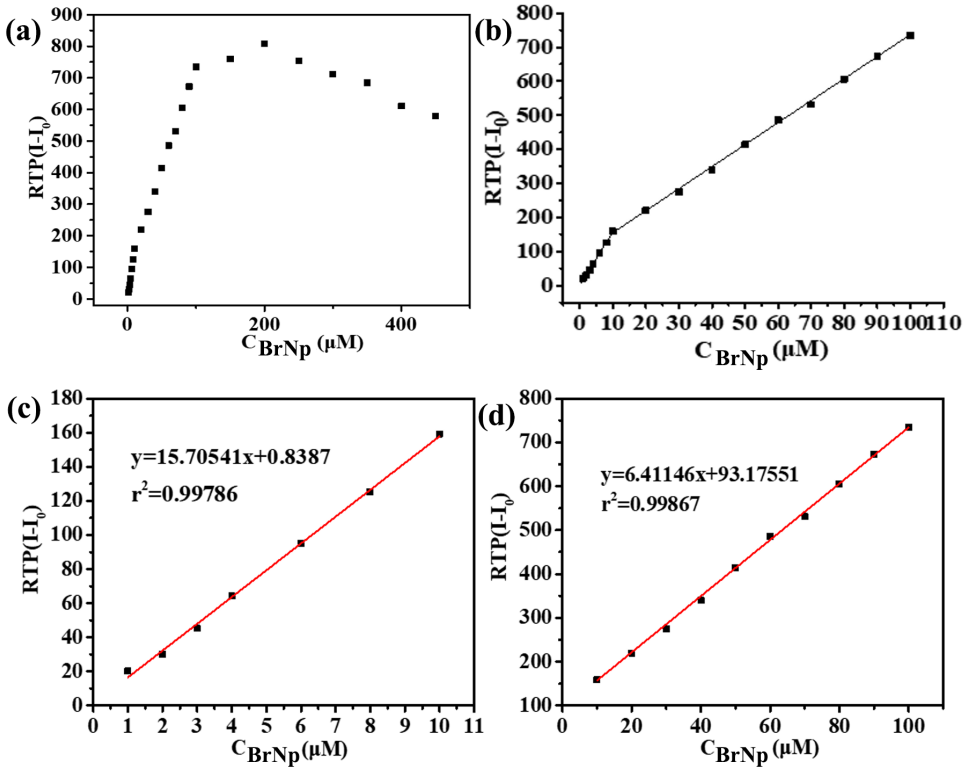

Figure 8 a, b) Changes in RTP intensity of different concentrations of BrNp in HmeQ[5]/DB gel (1.50 wt%, formic acid/water = 1/9, v/v), c) Linear fitting of BrNp concentration at the range of 1.0×10^{-6}- 1.0×10^{-5} mol / L, d) Linear fitting of BrNp concentration over the range 1.0×10^{-5} - 1.0×10^{-4} mol / L.

4. Conclusion

In summary, the HmeQ[5]/DB based hydrogel was obtained through a simple heating and cooling process. The structure and properties of the HmeQ[5]/DB based hydrogel were studied, and the results showed that the key driving force of the gelation process was hydrogen bonding and ion dipole interactions between the portal oxygen atom of the HmeQ[5]/DB host and the two amino groups of the DB guest, thereby forming fibrils, and the appropriate concentration of protons present promoted these port interactions. Then these fibers form fiber bundles through the outer wall interactions between the cucurbituril methyl and the guest DB, and finally a gel was formed. On this basis, a pure organic luminescence supramolecular gel was prepared by simply heating and cooling the mixed solution containing the phosphors **BrNp** and the HmeQ[5]/DB based hydrogel. Luminescence studies show that **BrNp** exists in the ordered microstructure of the HmeQ[5]/DB based hydrogels. The relatively rigid structure effectively avoids non-radiative transitions and shields the effects of oxygen and other quenchants. Based on the structural reversibility of the supramolecular gel, that is, the phase

transition of gel under thermal stimulation, the simultaneous fluorescence and phosphorescence emission of BRN dispersed in the gel exhibited an "on-off" switching effect. **BrNp** has good room temperature phosphorescence detection and analysis parameters in the HmeQ[5]/DB supramolecular gel. This shows that gel matrix can promote the detection of phosphorescent substances with high sensitivity. The research extends the application of cucurbit[*n*]urils, and reveals the potential application value in new phosphorescent soft materials. Such applications are in progress in our laboratory.

ACKNOWLEDGMENTS

This work was financially supported by the National Natural Science Foundation of China (No. 21861011), and the Science and Technology Fund of Guizhou Province (No. 2018-5781). CR thanks the University of Hull for support.

Declarations

Conflict of interest All authors declare that they have no conflict of interest to disclose.

REFERENCES

[1] Fu, J.; Panhuis, M. I. H. Hydrogel properties and applications. *J. Mater. Chem. B,* 2019, 7, 1523-1525

[2] Wang, Q.; Mynar, J. L.; Yoshida, M.; Lee, E.; M. Lee, Okuro, K.; Kinbara, K.; K. and Aida, T. High-water-content mouldable hydrogels by mixing clay and a dendritic molecular binder. *Nature,* 2010, 463, 339–343.

[3] Li, J.; Ji, C. D.; Lu, B. Z.; Rodin, M.; Paradies, J.; Yin, M. Z.; Kuckling, D., Dually Crosslinked Supramolecular Hydrogel for Cancer Biomarker Sensing. *Acs Appl Mater Inter* 2020, *12* (33), 36873-36881.

[4] Yan, L. W.; Li, G. Z.; Ye, Z. B.; Tian, F.; Zhang, S. H. Dual-responsive two-component supramolecular gels for self-healing materials and oil spill recovery. *Chem. Commun.,* 2014, 50, 14839-14842

[5] Zhang, Y.; Chen, Y.; Li, J. J.; Liang, L.; Liu, Y. Construction and Luminescent Behavior of Supramolecular Hydrogel with White-Light Emission. *Acta Chim. Sinica* 2018, *76*, 622—626

[6] J. W. Steed, Anion-tuned supramolecular gels: a natural evolution from urea supramolecular chemistry. *Chem. Soc. Rev.,* 2010, 39, 3686-3699.

[7] Sangeetha, N. M.; Maitra, U., Supramolecular gels: functions and uses. *Chem Soc Rev* 2005, *34* (10), 821-836.

18 Peppas, N. A.; Bures, P.; Leobandung, W.; Ichikawa, H. Hydrogels in pharmaceutical formulations. *Eur. J. Pharm. Biopharm*., 2000, 50, 27–46.

[8] Carretti, E.; Bonini, M.; Dei, L.; Berrie, B. H.; Angelova, L. V.; Baglioni, P.; Weiss, R. G., New frontiers in materials science for art conservation: responsive gels and beyond. *Acc Chem Res* 2010, *43* (6), 751-60.

[9] Appel, E. A.; del Barrio, J.; Loh, X. J.; and Scherman, O. A. Supramolecular polymeric hydrogel. *Chem. Soc. Rev.,* 2012, **41**, 6195–

6214

[10] Babu, S. S.; Praveen, V. K.; and Ajayaghosh, A. Functional π-Gelators and Their Applications. *Chem. Rev.,* 2014, 114, 1973-2129.

[11] Voorhaar, L.; Hoogenboom, R. Supramolecular polymer networks: hydrogels and bulk materials. *Chem. Soc. Rev.,* 2016, 45, 4013-4031

[12] Zhang, J.; Ma, P. X., Cyclodextrin-based supramolecular systems for drug delivery: recent progress and future perspective. *Adv Drug Deliv Rev* **2013,** *65* (9), 1215-33.

[13] Dai, X. Y.; Zhang, Y. Y.; Gao, L. N.; Bai, T.; Wang, W.; Cui, Y. L.; Liu, W. G. A Mechanically Strong, Highly Stable, Thermoplastic, and Self-Healable Supramolecular Polymer Hydrogel. *Adv. Mater*. **2015**, *27*, 3566-3571.

[14] Dong, R. J.; Pang, Y.; Su, Y.; Zhu, X. Y. Supramolecular hydrogels: synthesis, properties and their biomedical applications. *Biomater. Sci.,* 2015, 3, 937–954

[15] Panja, S.; Adams, D. J. Stimuli responsive dynamic transformations in supramolecular gels. *Chem. Soc. Rev.*, 2021, 50, 5165–5200

[16] Abdollahi, A.**;** Roghani-Mamaqani, H.**;** Razavi**,** B. Salami-Kalajahi, M.**;** The light-controlling of temperature-responsivity in stimuli-responsive polymers**.** *Polym. Chem.,* 2019, 10, 5686–5720.

[17] Zhang, Z. X.; Liu, X.; Xu, F. J.; Loh, X. J.; Kang, E. T.; Neoh, K. G.; Li, J., Pseudo-block copolymer based on star-shaped poly(N-isopropylacrylamide) with a beta-cyclodextrin core and guest-bearing PEG: Controlling thermoresponsivity through supramolecular self-assembly. *Macromolecules* **2008,** *41* (16), 5967-5970.

[18] Lin, R. L.; Liu, J. X.; Chen, K.; Redshaw, C. Supramolecular chemistry of substituted cucurbit[n]urils. *Inorg. Chem. Front.,* 2020, 7, 3217–3246

[19] Bhasikuttan, A. C.; Pal, H.; Mohanty, J. Cucurbit[n]uril based supramolecular assemblies: tunable physico-chemical properties and their prospects. *Chem. Commun.,* 2011, **47**, 9959–9971

[20] Lu, W.; Le, X. X.; Zhang, J. W.; Huang, Y. J. and Chen, T. Supramolecular shape memory hydrogels: a new bridge between stimuli-responsive polymers and supramolecular chemistry. *Chem. Soc. Rev.,* 2017, 46, 1284-1294

[21] Panja, S.; Adams, D. J.Stimuli responsive dynamic transformations in supramolecular gels. *Chem. Soc. Rev.*, 2021, 50, 5165–5200

[22] Liu, J.; Tan, C. S. Y.; Yu, Z. Y.; Li, N.; Abell, C.; Scherman, O. A. Tough Supramolecular Polymer Networks with Extreme Stretchability and Fast Room-Temperature Self-Healing. *Adv Mater* **2017,** *29* (22).1605325.

[23] Tan, C. S. Y.; Liu, J.; Groombridge, A. S.; Barrow, S. J.; Dreiss, C. A.; Scherman, O. A. Controlling Spatiotemporal Mechanics of Supramolecular Hydrogel Networks with Highly Branched Cucurbit[8]uril Polyrotaxanes. *Adv. Funct. Mater.* 2018, 28, 1702994

[24] Song, Q.; Gao, Y. F.; Xu, J. F.; Qin, B.; Serpe, M. J.; Zhang, X. Supramolecular Microgels Fabricated from Supramonomers. *ACS Macro Lett.* 2016, 5, 1084-1088

[25] Park, K. Min.; Roh, J. H.; Sung, G.; Murray, J.; Kim. K. M. Self-Healable Supramolecular Hydrogel Formed by Nor-SecoCucurbit[10]uril as a Supramolecular Crosslinker. *Chem. Asian J*. 2017, 12, 1461 – 1464

[26] Park, K. M.; Yang, J. A.; Jung, H.; Yeom, J.; Park, J. S.; Park, K. H.; Hoffman, A. S.; Hahn, S. K.; Kim, K. In Situ Supramolecular Assembly and Modular Modification of Hyaluronic Acid Hydrogels for 3D Cellular Engineering. *ACS Nano* 2012, 6, 2960-2968.

[27] Zou, L.; Braegelman, A. S.; Webber, M. J. Dynamic Supramolecular Hydrogels Spanning an Unprecedented Range of Host-Guest Affinity. *ACS Appl. Mater. Interfaces* 2019, 11, 5695-5700

[28] Hwang, I.; Jeon, W. S.; Kim, H. J.; Kim, D. W.; Kim, H.; Selvapalam, N.; Fujita, N.; Shinkai, S. J.; Kim. K. M. Cucurbit[7]uril: A Simple Macrocyclic, pH-Triggered Hydrogelator Exhibiting Guest-Induced Stimuli-Responsive Behavior. *Angew. Chem.* 2007, 119, 214 –217

[29] Buerklea, L.E.; Rowan, S. J. Supramolecular gels formed from multi-component low molecular weight speciesw. *Soc. Rev.,* 2012,

41, 6089–6102

[30] Ma, X.; Wang, J.; Tian, H. Assembling-Induced Emission: An Efficient Approach for Amorphous Metal-Free Organic Emitting Materials with Room Temperature Phosphorescence. *Acc. Chem. Res.* 2019, 52, 738-748

[31] DeRosa, C. A.; Seaman, S. A.; Mathew, A. S.; Gorick, C. M.; Fan, Z.; Demas, J. N.; Peirce, S. M.; Fraser, C. L. Oxygen sensing difluoroboron β-diketonate polylactide materials with funable dynamic ranges for wound imaging. *ACS Sens* 2016, 1, 1366-1373.

[32] Miao, Q.; Xie, C.; Zhen, X.; Lyu, Y.; Duan, H.; Liu, X.; Jokerst, J. V.; Pu, K. Molecular afterglow imaging with bright, biodegradable polymer nanoparticles. *Nat. Biotechnol.* 2017, 35, 1102.

[33] Gao, H. Q.; Gao, Z. Y.; Jiao, D.; Zhang, J. T.; Li, X. L.; Tang, Q. Y.; Shi, Y. and Ding, D. Boosting Room Temperature Phosphorescence Performance by Alkyl Modification for Intravital Orthotopic Lung Tumor Imaging. *Small* 2021, 17, 2005449

[34] Zhou, W. L.; Chen, Y.; Yu, Q. L.; Zhang, H. Y.; Liu, Z. X.; Dai, X.Y.; Li, J.J. & Liu, Y. Ultralong purely organic aqueous phosphorescence supramolecular polymer for targeted tumor cell imaging. *Nat. Commun*. 2020, 11:4655

[35] Gao, R.; Mei, X.; Yan, D.; Liang, R.; Wei, M. Nanophotosensitizer based on layered double hydroxide and isophthalic acid for singlet oxygenation and photodynamic therapy. *Nat. Commun.* 2018, 9, 2798.

[36] Xiao, B.; Wang, Q.; Zhang, S.; Li, X. Y.; Long, S. Q.; Xiao, Y.; Xiao, S.; Ni, X. L., Cucurbit[7]uril-anchored polymer vesicles enhance photosensitization in the nucleus. *J Mater Chem B* **2019,** *7* (39), 5966-5971.

[37] S. van Dun, C. Ottmann, L.-G. Milroy, L. Brunsveld, *J. Am. Chem. Soc.* 2017, 139, 13960 – 13968.

[38] Kim, K. L.; Sung, G.; Sim, J.; Murray, J.; Li, M.; Lee, A.; Shrinidhi, A.; Park, K. M.; Kim, K., Supramolecular latching system based on ultrastable synthetic binding pairs as versatile tools for protein imaging. *Nat Commun* **2018,** *9*.1712.

[39] Lu, L.B.; Yu, D.H.; Zhang, Y. Q.; Zhu, Q. J.; Xue, S. F.; Tao, Z. Supramolecular assemblies based on some new methyl-substituted cucurbit[5]urils through hydrogen bonding. *J. Mol. Struct.* 2008, 885, 70-75.

[40] Ni, X. L.; Xiao, X.; Cong, H.; Zhu, Q. J.; Xue, S. F.; Tao, Z. Self-Assemblies Based on the “Outer-Surface Interactions” of Cucurbit[n]urils: New Opportunities for Supramolecular Architectures and Materials. Acc. Chem. Res. 2014, 47, 1386-1395.

[41] Yuan, J.H.; Dong, X. L.; Zhang, B. B.; Zhou, Q.; Lu, S.; Wang, Q.; Liao, Y. G.; Yang, Y. J.; Wang, H. Tunable dual emission of fluorescence- phosphorescence at room temperature based on pure organic supramolecular gels. *Dyes and Pigments* 181 (2020) 108506